

Electronic and structural properties of carbon nanotubes modulated by external strain

Wan-Sheng Su^{a)}

National Center for High-Performance Computing, Taichung 40763, Taiwan

(Received 27 March 2013; accepted 12 June 2013; published online 28 June 2013)

Responses of work functions to uniaxial strain on infinite-length single-walled armchair (AC) [(2, 2) and (7, 7)] and zigzag (ZZ) [(3, 0) and (12, 0)] carbon nanotubes (CNTs) are investigated based on density functional theory. It is found that as strain increases, the work function of ZZ (3, 0) tubes decreases monotonically from 6.2 to 5.7 eV, whereas that of AC (2, 2) tubes varies between 4.6 and 5.3 eV in a somewhat complicated manner. For ZZ (12, 0) and AC (7, 7) tubes with large diameters, the work function of ZZ (12, 0) changes almost linearly from 4.2 to 4.8 eV, while for AC (7, 7) work function values grow monotonically from 4.1 to 4.7 eV. The energy band changes provide a qualitative understanding of how work function is affected by the uniaxial strain. Our findings are helpful not only for understanding the electronic properties of strained CNTs but also open the possibility of potential applications in CNT-based electronics devices. © 2013 AIP Publishing LLC. [<http://dx.doi.org/10.1063/1.4812478>]

I. INTRODUCTION

Carbon nanotubes (CNTs) can be viewed as graphene sheets rolled up into cylindrical structures. Since their discovery in 1991,¹ the peculiar electronic properties of such hollow nanostructures have gained growing attention from scientists and researchers. CNTs show great potential for a variety of technological applications due to their novel physical properties. Depending on radius and chirality, a single-walled carbon nanotube (SWCNT) can behave as either metallic or semiconducting.² The (n, m) SWCNT is classified as a metal when $(2n + m)/3$ is an integer; otherwise, it is a semiconductor. These results, predicted on the basis of the zone-folding (ZF) approach,³ were found to be influenced by curvature effects, the misorientation of 2pz orbitals and the hybridization of π and σ states. As such, small modifications have arisen in the simple three-multiple rule, re-classifying the CNT for $2n + m = 3I$ into two categories. The (n, n) armchair (AC) CNTs remain gapless, whereas for CNTs where $n \neq m$, an energy gap opening whose magnitude is proportional to $1/r^2$ (r being the nanotube radius) is displayed.

Understanding the electronic properties of CNTs is an important issue in integrating nanotubes into devices. The use of CNTs as field emitters in flat panel displays⁴ is one of the most promising applications of CNTs. The CNT work function is a very important parameter in judging its field-emission properties, and many researchers have attempted to measure these work functions.^{5–8} For instance, Shiraishi and Ata⁷ measured the work function of SWCNTs to be 5.05 eV using the photoelectron emission method. Su *et al.*⁹ showed that the work function of armchair SWCNTs is not only close to that of a graphene (~ 4.48 eV), but also independent of tube diameter. For a zigzag (ZZ) SWCNT with a diameter

greater than 10 Å, its work function value is also close to that of graphene. However, for a zigzag SWCNT with diameter less than 10 Å, work function increases dramatically as the diameter decreases.

Tuning the electronic properties of SWCNTs has been a subject of interest to both experimental and theoretical researchers with the motivation of finding possible applications. In addition to doping with various types of foreign atoms^{10–13} and adsorption of foreign atoms or molecules,^{14,15} another effective way to widen their application possibilities is by applying external strain. Mechanical strain often gives rise to surprising effects on the electronic properties of carbon nanomaterials, often drastically changing the intrinsic properties of CNTs. Numerous experimental studies have been carried out on this phenomenon. For instance, using an atomic force microscope, CNTs can be radially deformed, resulting in significant changes in their transport characteristics due to metal-semiconductor and/or semiconductor-metal transitions.^{16–18} However, it is very difficult to measure the mechanical properties of CNTs directly due to their nanoscale size. Accordingly, many theoretical techniques have been applied to investigate the mechanical properties of CNTs. Using a sp^3 tight-binding model, Ding *et al.*¹⁹ have shown that semiconductor-metal-semiconductor phase transitions are observed for primary metallic non-armchair nanotubes, while the application of uniaxial strain does not cause a band gap for an armchair tube. Using first-principle calculations, direct atomic and electronic configurations of deformed CNTs were performed by Iwami *et al.*,²⁰ who reported that the effect of deformation along the tube axis on an armchair tube causes changes in energy bands and electron charge density distribution. In addition, the presence of a natural torsion in small diameter chiral SWCNTs has been studied by Vercosa *et al.*,²¹ and they reported the presence of such natural torsion has several important implications on the physics of nanotubes, such as a further opening of the

^{a)}Author to whom correspondence should be addressed. Electronic mail: wssu@nchc.narl.org.tw

minigaps in metallic SWCNTs, changing the optical transition energies, and having implications on the breaking of the pure translational symmetry of the chiral nanotubes. Because our study is concerned with non-chiral rather than chiral nanotubes, however, this torsion effect has no bearing on the SWCNTs here.

CNTs with small diameters display many attractive properties, including anisotropic optical adsorption spectra²² and superconductivity originating from a Peierls distortion.^{23,24} Recently, ultra small (2, 2) and (3, 0) CNTs were verified to exist with stable mechanical structures as a SWCNT or being formed inside a multiwalled carbon nanotubes (MWCNTs) at room temperature.^{25–28} Relative to CNTs of a large tube diameter, these ultra small nanotubes exhibit the unusual characteristic of excellent field emission properties due to their large curvature effect. Moreover, since the mechanical deformations are notable during the process of building CNT-based devices, it is of interest and important to understand the electronic properties of strained CNTs in order to have a complete understanding of how individual CNTs behave under uniaxial strain. Thus, in this study, we are concerned with individual SWCNTs of relatively small tube diameter and report on their work function modulation by application of uniaxial strain. The corresponding geometric structures and electronic properties are further analyzed and compared with those of SWCNTs with large diameters.

II. ELECTRONIC STRUCTURES

The first-principle calculations are performed in the framework of the density functional theory (DFT)²⁹ implemented by the VASP code.^{30,31} Projector augmented wave (PAW) pseudopotentials³² and local density approximation (LDA) exchange-correlation potential are utilized. A plane-wave cut-off of 500 eV is used in the calculations. All atoms are fully relaxed until the residual force on each atom is less than 0.02 eV/Å. To simulate the strain effect on the systems, we computed a series of expanded and reduced lattice constants (i.e., increase and decrease in the length of the tube) along the axial direction of the tube that mimics the application of uniaxial stress parallel to the tube-axis direction.³³ Here, the uniaxial stress was imposed uniformly, and the corresponding strain (ε) was defined as $\varepsilon = \Delta\ell/\ell$, where ℓ is the initial length of the unstrained structures and $\Delta\ell$ is the change in length due to the strain (stretching or compression). Figure 1 illustrates models of the studied system with manipulated strains, either tensile or compressive. The work functions are determined from the difference between the Fermi level and the vacuum level. The vacuum level was defined as the average potential outside the material where the potential approaches a constant value. In the case of semiconducting nanotubes, the Fermi level was chosen at the middle of the bandgap.

A. Zone-folding methods

The zone-folding scheme is a computationally cost-effective method for the investigation of nanotube electronic structures. In this zone-folding method, the electronic structures of a planar graphite sheet are first obtained by the first-

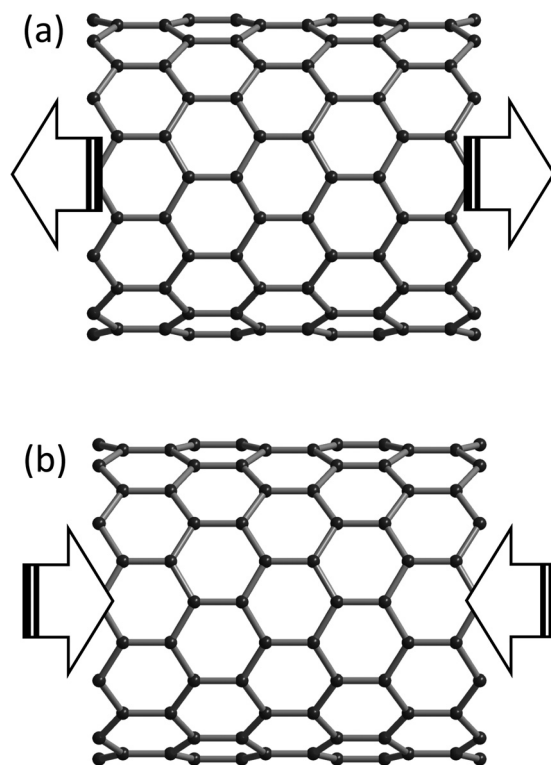


FIG. 1. Illustration of strained systems for (a) tensile and (b) compressive carbon nanotubes. Here, tensile and compressive, respectively, mean uniformly stretching or compressing the length of the tube.

principles method. Next, the obtained first-principles band structures of the graphite sheet are combined with the zone-folding scheme to generate the electronic structures of the carbon nanotubes. A set of band structures for armchair and zigzag nanotubes can be obtained by rolling up the graphite sheet, the obtained electronic structures of the carbon nanotubes are shown in Fig. 2 (dashed line). Zone-folding calculations on the armchair and zigzag nanotubes of up to (12, 12) and (15, 0) nanotubes, respectively, have been performed in this work, but only the electronic structures of the smaller diameter (2, 2), (3, 0), (7, 7), (12, 0) nanotubes are plotted. Obviously, the effects of nanotube curvatures are entirely ignored in this approach.

B. First-principles methods

To fully illustrate the electronic structures of the carbon nanotubes, first-principles calculations are performed. The

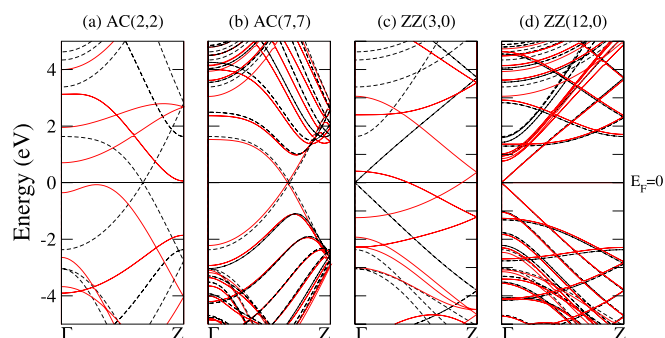


FIG. 2. Band structures of zone-folding (dashed line) and LDA (solid line) results for AC and ZZ tubes.

electronic structures of the carbon nanotubes obtained by the first-principles method are shown in Fig. 2 (solid line). Clearly, as demonstrated in Fig. 2, the band structures of ultra-small (2, 2) and (3, 0) tubes obtained by first-principles and zone-folding methods are very different, showing that for nanotubes with ultra-small diameters, the zone-folding approach clearly fails because of the large curvature effects neglected in this scheme. As a result, in this work, we employed the first-principles method to illustrate the full features of the electronic structures of carbon nanotubes.

III. RESULTS AND DISCUSSION

Figure 3 depicts the computed total energy per atom as a function of the strain (ε) for SWCNTs of different tube diameters, whether in the AC or ZZ form. From this figure, one can see that with respect to other tubes, only the AC (2, 2) tube possesses two ground states, denoted as G_0 and G_1 , with the former having a lower total energy than the latter. It should be stressed that G_0 is a semiconductor (S), and G_1 behaves like a metal (M). This is in reasonable agreement with a recent report by Tang *et al.*²²

The following presents the corresponding geometric structures for both (2, 2) and (3, 0) small tubes. Figure 4 displays two types of bonding (denoted as d_1 and d_2) and two bond angles (denoted as θ_1 and θ_2) for AC (2, 2) and ZZ (3, 0) CNTs. For AC tubes, d_1 bonding is a C-C bond along the tube ring and is vertical to the tube axis, while for ZZ, d_1 is parallel to the tube axis. It is noted that for carbon, the values of the C-C bond length and bond angles in monolayer graphite sheet (sp^2 hybridization) and in diamond (sp^3 hybridization) are, respectively, 1.42 Å, 120° and 1.54 Å, 109.47°.

The optimized geometric structures of (2, 2) and (3, 0) tubes with strains of d_1 , d_2 , θ_1 , and θ_2 are explored in Fig. 5. First, we discuss the different bond lengths d_1 and d_2 for both (2, 2) and (3, 0) tubes. For the (2, 2) tubes, when strain changes from compressive (negative) to tensile (positive), the values of d_1 decrease, whereas the opposite holds true in d_2 . Note that d_2 is larger than d_1 with the strain greater than the turning point of $\sim -3.5\%$, with d_1 becoming larger than

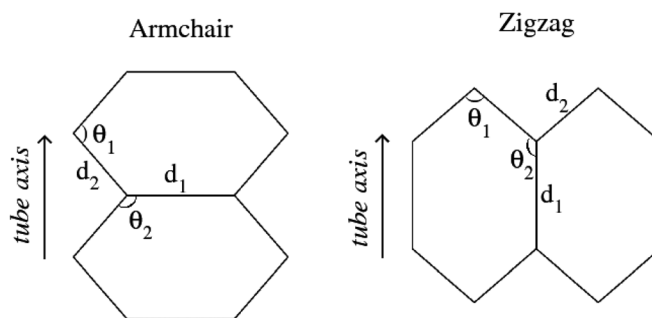


FIG. 4. Two types of bond length (denoted as d_1 and d_2) and bond angle (denoted as θ_1 and θ_2) for AC (2, 2) and ZZ (3, 0) CNTs.

d_2 at strain smaller than the turning point of $\sim -3.5\%$. Different from the (2, 2) tubes, the values of both d_1 and d_2 for (3, 0) tubes increase linearly with applied strains from compressive to tensile, where d_2 is always larger than d_1 . Next, the behavior of bond angles θ_1 and θ_2 with various strains is presented. For (3, 0) tubes, with applied strains from compressive to tensile, the values of θ_1 reduce linearly, whereas those of θ_2 show an increasing trend, with θ_2 larger than θ_1 . Compared to (3, 0) tubes, (2, 2) tubes display opposite directional trends for θ_1 and θ_2 —though nonlinear—with θ_1 larger than θ_2 as strains from compressive to tensile are applied. Finally, as can be seen in Fig. 5, results show that bond lengths of d_1 and d_2 for the G_0 state of (2, 2) tubes are, respectively, about 1.37 and 1.48 Å for bond angles of θ_1 and θ_2 , 119.6° and 110.8°, respectively. These values imply a strong mixture of the sp^2 and sp^3 hybridizations. Compared to the G_0 state, the G_1 state exhibits a different trend such that d_1 and d_2 are 1.45 and 1.44 Å, while θ_1 and θ_2 are 117.9° and 111.4°. In the case of the (3, 0) tubes, calculations demonstrate that bond lengths of d_1 and d_2 for ground state are, respectively, about 1.39 and 1.47 Å. Bond angles of θ_1 and θ_2 are about 99.8° and 118.0°.

Strain dependences of work function for SWCNTs of different diameters in the AC and ZZ conformations are plotted in Fig. 6. As mentioned above, the band structures of (2, 2) and (3, 0) tubes are given by the ZF approach with a

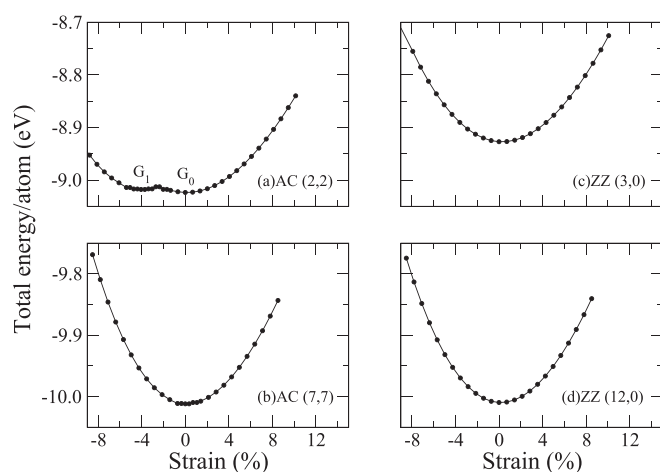


FIG. 3. Strain effects on total energy of (a) AC (2, 2), (b) AC (7, 7), (c) ZZ (3, 0), and (d) ZZ (12, 0) nanotubes.

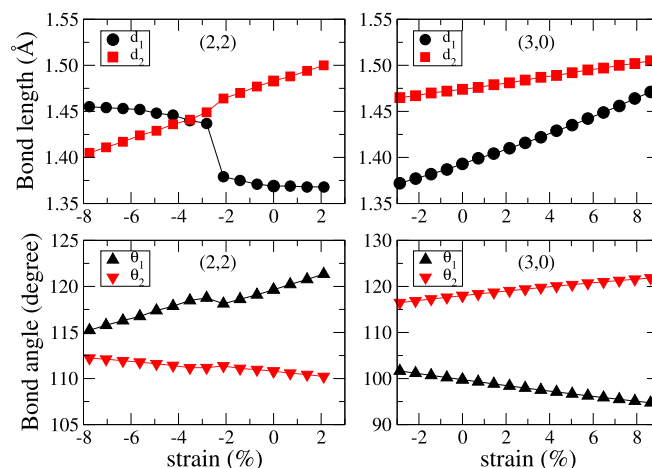


FIG. 5. Two types of bond length (d_1 and d_2) and bond angles (θ_1 and θ_2) against strain for both armchair (2, 2) and zigzag (3, 0) tubes. θ_1 is the angle between two d_2 bond lengths, and θ_2 is the angle between d_1 and d_2 .

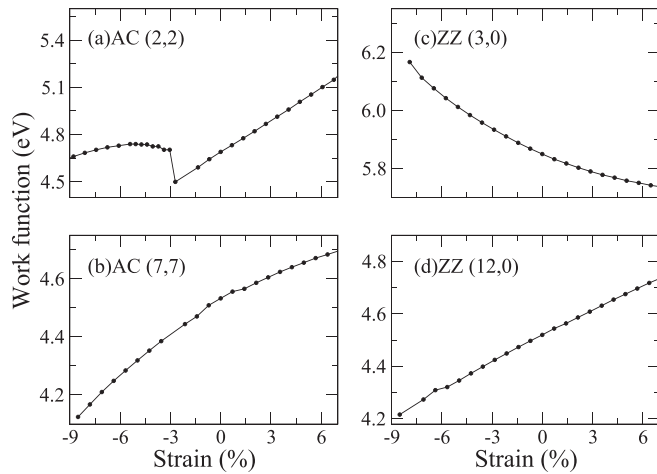


FIG. 6. Work function versus strain for (a) AC (2, 2), (b) AC (7, 7), (c) ZZ (3, 0), and (d) ZZ (12, 0) CNTs. In the case of a semiconducting nanotube, the Fermi level was chosen at the midgap.

modification due to the large curvature effects. Clearly, such an effect results in a small energy gap of ~ 0.13 eV for the (2, 2) tube, so a higher work function than the (7, 7) tube would be expected due to the extra energy needed to overcome this energy barrier and emit electrons to the vacuum level. However, for (3, 0) tubes, such a curvature effect induces a downshift of the Fermi level relative to the vacuum level and thus enhances the work function. Therefore, the work function value of the (3, 0) tube is larger than that of the (12, 0) one. We found that strain has great influences on work functions of both SWCNTs of different diameters. The work function of ZZ (3, 0) tubes decreases monotonically from 6.2 to 5.7 eV, whereas that of AC (2, 2) tubes varies

between 4.6 and 5.3 eV, though in a more complicated manner. With the growth of tube diameter, the work function of ZZ (12, 0) changes almost linearly from 4.2 to 4.8 eV, while for AC (7, 7) its work function value grows monotonically from 4.1 to 4.7 eV. These findings demonstrate that tuning strain may be an effective way to control work functions of CNTs, which is important for future design of CNT-based nanodevices.

Compared to nanotubes of large diameter, the response of work function to strain for small tubes is quite interesting. To qualitatively understand this phenomenon, some band structures with applied strains are calculated, as shown in Fig. 7. It is obvious that the strain causes changes in the energy band structures. In the case of the (2, 2) tube, one can see from Fig. 7(a) that with compressive strain, one of the bands (red lines) from the valence region is systematically shifted up and two of the conduction bands (blue lines) shift down towards the Fermi level, and as a result, one conduction band and the valence band cross at a value of $\epsilon = -2.7\%$. However, with tensile strain, one of the bands from the valence region systematically shifts down and two of the conduction bands shift up away from the Fermi level and as a result, the band gap becomes larger with the growth of strain. The crossing band structure in compressive strain causes the changes in the bond length and work function of AC (2, 2) at $\epsilon = -2.7\%$, from non-linear to linear relationship in the work function and for bond lengths d_2 becoming greater than d_1 . Fig. 8 shows a progressively stronger strain on the (2, 2) tube, indicating that the cross does not occur until $\epsilon = -2.7\%$.

In the case of the (3, 0) tubes, Fig. 7(c) demonstrates that with increasing compressive strain, the two sets of bands

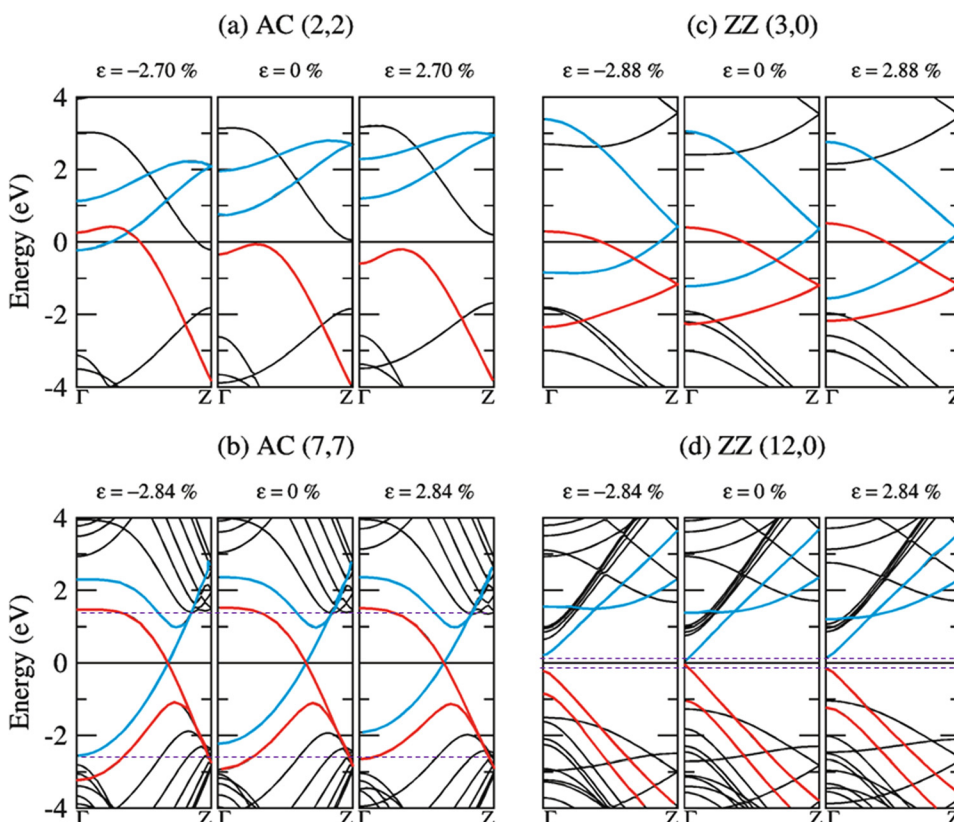


FIG. 7. Band structures of (a) AC (2, 2), (b) AC (7, 7), (c) ZZ (3, 0), and (d) ZZ (12, 0) CNTs versus various strains.

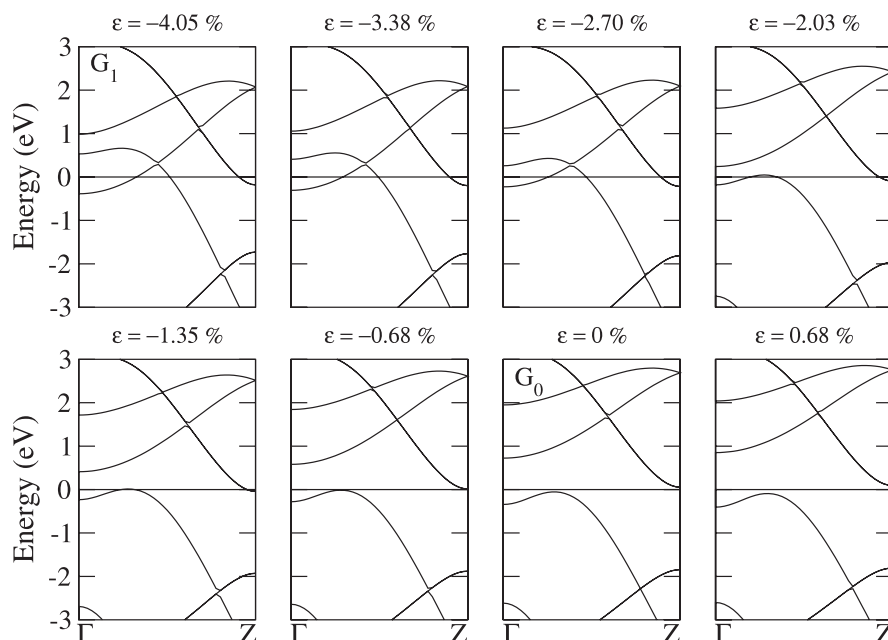


FIG. 8. Change of the band structure of AC (2, 2) caused by applied strain. It is noted that G_0 state is a semiconductor, whereas G_1 state behaves like a metal.

(in blue and red) become farther apart, with the red bands lowering in energy as the blue bands increase in energy. During tensile strain, however, they similarly spread apart, but the blue bands become lower in energy while the red bands increase. As for the cases of tubes with large diameter, the influence on the energy band from the strain displays quite different behaviors for AC (7, 7) and ZZ (12, 0) tubes.^{20,34} For the AC (7, 7) tube, the compressive strain induces one of the blue bands to shift below Fermi level and one of the red bands to shift above Fermi level, resulting in an increase in energy window between these two bands at the gamma (Γ) point. In contrast, tensile strain induces a lower value in such an energy window by shifts in the opposite direction as compressive strain. In other words, strain induces the shift of the intersection of one valence and one conduction bands at the Fermi level along the Γ Z direction. While for ZZ (12, 0) tube, such a strain effect causes an oscillation in bandgap, different to that which occurs in the case of AC (7, 7) tube. Obviously, an applied strain causes the changes in energy band, which alters the corresponding Fermi energy, and in turn indeed causes the variations in the work function values. These findings suggest that the strain effect plays a key role in significantly tuning nanotube work function, and may give rise to potentially useful variations in nano-circuits and components of CNT-based electronics device applications.

IV. CONCLUSIONS

The calculations of total energy versus strain reveal that only the AC (2, 2) tube exhibits two metastable ground states, one of which is semiconducting at $\varepsilon=0$ while the other is metallic at $\varepsilon=-4.05\%$. This fact implies a semiconductor-metal transition found in the case of AC (2, 2) compared to other tubes due to the presence of external strains. Moreover, the effects of the strain show an influence on the work functions of small tubes, with AC (2, 2) tube displaying behavior quite different from ZZ (3, 0) tube. Such resulting deviations

in work function can be qualitatively explained by the changes in energy band due to the presence of given applied strains. Our findings are helpful not only for understanding the electronic properties of strained CNTs but also for optimal design of the CNTs for nano-circuits and components of CNT-based electronics devices; for instance, designing circuits composed of two concentric nanotubes of different radii, such as (2, 2) @ (7, 7) and (3, 0) @ (12, 0), can be expected to show dramatic changes in the electronic properties of the inner and outer tubes which in turn influence the conductivity of the system due to the presence of strains.

ACKNOWLEDGMENTS

The author would like to thank the National Science Council (NSC) of Taiwan for financially supporting this research under Contract Nos. NSC-99-2112-M-001-037-MY2 and NSC-101-2112-M-492-001-MY3. Support from the National Centers for Theoretical Sciences (South) and High-performance Computing of Taiwan by providing significant computing resources to facilitate this research is also gratefully acknowledged.

- ¹S. Iijima, *Nature (London)* **354**, 56 (1991).
- ²R. Saito, M. Fujita, G. Dresselhaus, and M. S. Dresselhaus, *Appl. Phys. Lett.* **60**, 2204 (1992); *Phys. Rev. B* **46**, 1804 (1992).
- ³N. Hamada, S. Sawada, and A. Oshiyama, *Phys. Rev. Lett.* **68**, 1579 (1992).
- ⁴Q. H. Wang, A. A. Setlur, J. M. Lauerhaas, J. Y. Dai, E. W. Seelig, and R. P. H. Chang, *Appl. Phys. Lett.* **72**, 2912 (1998).
- ⁵S. Suzuki, C. Bower, Y. Watanabe, and O. Zhou, *Appl. Phys. Lett.* **76**, 4007 (2000).
- ⁶R. Gao, Z. Pan, and Z. L. Wang, *Appl. Phys. Lett.* **78**, 1757 (2001).
- ⁷M. Shiraishi and M. Ata, *Carbon* **39**, 1913 (2001).
- ⁸S. Suzuki, Y. Watanabe, Y. Homma, S. Y. Fukuba, S. Heun, and A. Locatelli, *Appl. Phys. Lett.* **85**, 127 (2004).
- ⁹W. S. Su, T. C. Leung, and C. T. Chan, *Phys. Rev. B* **76**, 235413 (2007).
- ¹⁰D. Golberg, Y. Bando, W. Han, K. Kurashima, and T. Sato, *Chem. Phys. Lett.* **308**, 337 (1999).
- ¹¹F. Villalpando-Paez, A. Zamudio, A. L. Elias, H. Son, E. B. Barros, S. G. Chou, Y. A. Kim, H. Muramatsu, T. Hayashi, J. Kong, H. Terrones,

- G. Dresselhaus, M. Endo, M. Terrones, and M. S. Dresselhaus, *Chem. Phys. Lett.* **424**, 345 (2006).
- ¹²S. S. Yu, Q. B. Wen, W. T. Zheng, and Q. Jiang, *Nanotechnology* **18**, 165702 (2007).
- ¹³W. S. Su, C. P. Chang, M. F. Lin, and T. L. Li, *J. Appl. Phys.* **110**, 014312 (2011).
- ¹⁴L. Qiao, W. T. Zheng, Q. B. Wen, and Q. Jiang, *Nanotechnology* **18**, 155707 (2007).
- ¹⁵S. F. Xu, G. Yuan, C. Li, W. H. Liu, and H. Mimura, *J. Phys. Chem. C* **115**, 8928 (2011).
- ¹⁶E. D. Minot, Y. Yaish, V. Sazonova, J. Y. Park, M. Brink, and P. L. McEuen, *Phys. Rev. Lett.* **90**, 156401 (2003).
- ¹⁷T. W. Tomblor, C. Zhou, L. Alexseyev, J. Kong, H. Dai, L. Liu, C. S. Jayanthi, M. Tang, and S. Wu, *Nature* **405**, 769 (2000).
- ¹⁸A. P. M. Barboza, A. P. Gomes, B. S. Archanjo, P. T. Araujo, A. Jorio, A. S. Ferlauto, M. S. C. Mazzoni, H. Chacham, and B. R. A. Neves, *Phys. Rev. Lett.* **100**, 256804 (2008).
- ¹⁹J. W. Ding, X. H. Yan, J. X. Cao, D. L. Wang, Y. Tang, and Q. B. Yang, *J. Phys.: Condens. Matter* **15**, L439 (2003).
- ²⁰K. Iwami, H. Goto, K. Hirose, and T. Ono, *Sci. Technol. Adv. Matter.* **8**, 200 (2007).
- ²¹D. G. Vercosa, E. B. Barros, A. G. Souza Filho, J. Mendes Filho, Ge. G. Samsonidze, R. Saito, and M. S. Dresselhaus, *Phys. Rev. B* **81**, 165430 (2010).
- ²²Z. M. Li, Z. K. Tang, H. J. Liu, N. Wang, C. T. Chan, R. Saito, S. Okada, G. D. Li, J. S. Chen, N. Nagasawa, and S. Tsuda, *Phys. Rev. Lett.* **87**, 127401 (2001).
- ²³Z. K. Tang, L. Zhang, N. Wang, X. X. Zhang, G. H. Wen, G. D. Li, J. N. Wang, C. T. Chan, and P. Sheng, *Science* **292**, 2462 (2001).
- ²⁴D. Connétable, G. M. Rignanese, J. C. Charlier, and X. Blase, *Phys. Rev. Lett.* **94**, 015503 (2005).
- ²⁵L. M. Peng, Z. L. Zhang, Z. Q. Xue, Q. D. Wu, Z. N. Gu, and D. G. Pettifor, *Phys. Rev. Lett.* **85**, 3249 (2000).
- ²⁶X. Zhao, Y. Liu, S. Inoue, T. Suzuki, R. O. Jones, and Y. Ando, *Phys. Rev. Lett.* **92**, 125502 (2004).
- ²⁷Y. L. Mao, X. H. Yan, Y. Xiao, J. Xiang, Y. R. Yang, and H. L. Yu, *Nanotechnology* **15**, 1000 (2004).
- ²⁸Y. L. Mao, X. H. Yan, Y. Xiao, J. Xiang, Y. R. Yang, and H. L. Yu, *Phys. Rev. B* **71**, 033404 (2005).
- ²⁹W. Kohn and L. J. Sham, *Phys. Rev.* **140**, A1133 (1965).
- ³⁰G. Kresse and D. Joubert, *Phys. Rev. B* **59**, 1758 (1999).
- ³¹G. Kresse and J. Furthmüller, *Phys. Rev. B* **54**, 11169 (1996).
- ³²P. E. Blöchl, *Phys. Rev. B* **50**, 17953 (1994).
- ³³W. S. Su, F. C. Chuang, K. M. Lin, and T. C. Leung, *J. Vac. Sci. Technol. A* **28**, 1366 (2010).
- ³⁴S. Sreekala, X. H. Peng, P. M. Ajayan, and S. K. Nayak, *Phys. Rev. B* **77**, 155434 (2008).